Available online at www.sciencedirect.com

ScienceDirect

journal homepage: www.jfda-online.com

Original Article

Utilizing proteomic approach to identify nuclear translocation related serine kinase phosphorylation site of GNMT as downstream effector for benzo[a]pyrene

Ming-Hui Yang [a,b,c,d], *Chen-Chung Liao* [e], *Jung-Hsien Hung* [b], *Xiu-Ting Lai* [f], *Chia-Hung Yen* [b,g,h,i,**], *Yi-Ming Arthur Chen* [b,c,*]

[a] *Institute of Biological Chemistry, Academia Sinica, Taipei, 11529, Taiwan*
[b] *Center for Infectious Disease and Cancer Research (CICAR), Kaohsiung Medical University, Kaohsiung 80708, Taiwan*
[c] *Master Program in Clinical Pharmacogenomics and Pharmacoproteomics, College of Pharmacy, Taipei Medical University, Taipei, 11031, Taiwan*
[d] *Research Center for Environmental Medicine, Kaohsiung Medical University, Kaohsiung 807, Taiwan*
[e] *Proteomics Research Center, National Yang-Ming University, Taipei 11221, Taiwan*
[f] *Institute of Microbiology and Immunology, National Yang-Ming University, Taipei 11221, Taiwan*
[g] *Graduate Institute of Natural Products, College of Pharmacy, Kaohsiung Medical University, Kaohsiung 80708, Taiwan*
[h] *Research Center for Natural products and Drug Development, Kaohsiung Medical University, Kaohsiung, Taiwan*
[i] *Department of Medical Research, Kaohsiung Medical University Hospital, Kaohsiung, Taiwan*

ARTICLE INFO

Article history:
Received 2 July 2018
Received in revised form
17 December 2018
Accepted 20 December 2018
Available online 8 January 2019

Keywords:
Benzo(a)pyrene
GNMT
Phosphorylation

ABSTRACT

Glycine N-methyltransferase (GNMT) protein is highly expressed in certain tissues, such as liver, pancreas, and prostate. GNMT serves multiple roles which include a methyl group transfer enzyme and a liver tumor suppressor. Benzo(a)pyrene (BaP), a family member of polycyclic aromatic hydrocarbon (PAH), is a known environmental carcinogen found in coal tar, tobacco smoke, barbecued food and incomplete combustion of auto fuel. BaP recruits cytochrome P450 to transform itself into benzo(a)pyrene-7,8-diol-9,10-epoxide (B(a)PDE), which covalently interacts with DNA causing tumorigenesis. BaP can be detoxified through GNMT and induces GNMT translocation into the cellular nucleus. GNMT translocation is accompanied by phosphorylation, but the role of phosphorylation in GNMT remains to be explored. Using liquid chromatography coupled with tandem mass spectrometry, this study identified serine 9 of GNMT as the phosphorylation site upon BaP treatment. When serine 9 was mutated and lost the capability to be phosphorylated, the occurrence of BaP-induced GNMT nuclear translocation was dramatically decreased. Also, this mutant from of GNMT lost the ability of phosphorylation and increased cytochrome P450 1A1 (Cyp1a) expression upon BaP treatment. In addition, protein kinase C (PKC) and c-

* *Corresponding author*. No. 100, Shih-Chuan Ist Rd, Kaohsiung City, 80708, Taiwan. Fax: +886 7 3222783.
** *Corresponding author*.
E-mail addresses: chyen@kmu.edu.tw (C.-H. Yen), arthur@kmu.edu.tw (Y.-M.A. Chen).
https://doi.org/10.1016/j.jfda.2018.12.007
1021-9498/Copyright © 2019, Food and Drug Administration, Taiwan. Published by Elsevier Taiwan LLC. This is an open access article under the CC BY-NC-ND license (http://creativecommons.org/licenses/by-nc-nd/4.0/).

Jun NH2-terminal kinase (JNK) may be required for such phosphorylation. Further characterization of phosphorylated GNMT for its link to BaP may bring new insights into chemical detoxification.

Copyright © 2019, Food and Drug Administration, Taiwan. Published by Elsevier Taiwan LLC. This is an open access article under the CC BY-NC-ND license (http://creativecommons.org/licenses/by-nc-nd/4.0/).

1. Introduction

Polycyclic aromatic hydrocarbons (PAHs) are organic pollutants commonly produced by burning solid fuels or combustion of tobacco [1]. PAHs accumulate in soils easily and its suggested environmental assessment indicator is benzo(a)pyrene (BaP) [2]. BaP is a common mutagen and carcinogen in cigarette smoke, and its metabolism is via CYP1A1 (cytochrome P-4501A1) resulting a final product of benzo(a)pyrene- 7,8-diol-9, 10-epoxide (B(a)PDE), which binds to DNA and forms a BPDE-DNA covalent bond (BPDE-DNA adducts). These BPDE-DNA adducts cause damage to DNA and promote cancer [3–6].

The Glycine N-methyltransferase (GNMT) gene is located on chromosome 6 and its expressed protein has a molecular weight of 32 kDa. GNMT exists in cells usually as a homotetramer and has multiple functions including regulation of the ratio between S-adenosylmethionine (SAMe) and S-adenosylhomocystine (SAH) and acting as a major folate-binding protein [7,8]. GNMT comprises about 1–3% of cytosolic proteins in the liver and may serve as a liver tumor suppressor because knockout of this gene in mice leads to the progress of fatty liver, fibrosis and hepatocellular carcinoma [9]. In addition, this GNMT knockout mouse model has been applied as a screening tool to identify proteins related to tumor progression and as a strategy to discover missing proteins [10]. Gene-wise, higher GNMT promoter activity genotype workers were found to have fewer oxidative damaged DNA products [11]. All the results support that GNMT not only has an enzyme activity but also plays an important protective role against tumor formation.

In general, GNMT locates at cytosol but may be induced for translocation to nucleus by aristolochic acids type I (AAI), aflatoxin B1 (AFB1) and BaP [12–14]. Moreover, GNMT shows protective effects against the cytotoxicity and carcinogenicity of AAI, aflatoxin B1 (AFB1) and BaP in vitro and in vivo [12–14]. This study aims to identify the GNMT phosphorylation site upon BaP treatment and its influence. To investigate the effects of BaP on GNMT phosphorylation, we first employed the liquid chromatography-tandem mass spectrometry (LC-MS/MS) method to identify the phosphorylation site of GNMT induced by BaP. We also utilized molecular biology approaches to show that this phosphorylation site was associated with nuclear translocation of GNMT as well as changes of physiological activities.

2. Methods

2.1. Cell culture, transfection and viability assays

Embryonic kidney cell line HEK-293T and human liver cancer cell lines Huh7 and HepG2 were cultured in Dulbecco's Modified Eagle's Medium (DMEM) (Gibco BRL, Grand Island, NY, USA) with 10% heat-inactivated fetal bovine serum (HyClone, Logan, UT, USA), penicillin (100 U/mL), streptomycin (100 μg/ml), nonessential amino acids (0.1 mM/L) and L-glutamine (2 mM/L) in a humidified incubator with 5% CO_2. Lentivirus-infected cells were grown in complete DMEM supplemented with 1 μg/ml puromycin (Sigma–Aldrich, St. Louis, MO, USA) alone. Stable cells were grown in DMEM supplemented with 1 μg/mL puromycin. Plasmid DNA was transfected by using TurboFect Reagent (Thermo Fisher Scientific, Rockford, lL, USA). pGNMT-Flag construct has been described previously [14]. The mutant (S9A) was generated by site-directed mutagenesis using pCMV-GNMT-Flag as the template (Phusion SDM kit, Thermo Scientific). The primer sequences of S9A are (Forward) 5′-GTGTACCGGACCCGCGCCCTGGGGGTGGCGGCC-3′ and (Reverse) 5′-GGCCGCCACCCCCAGGGCGCGGGTCCGGTACAC -3′.

All transfections were performed according to the manufacturer's instructions. Forty-eight hours after transfection, cells were treated with different concentrations (1–10 μM) of BaP (Sigma–Aldrich, St. Louis, MO, USA) dissolved in DMSO (Nacalaitesque, Osaka, Japan) for 1–16 h. Treated cells were subjected to either indirect immunofluorescent assay, co-immunoprecipitation or immunoblotting. To produce a negative control, 0.1% DMSO was added to the cell culture. For cell viability assays, cells were seeded in a 96-well plate in triplicate and treated with DMSO or BaP for the indicated time. Then, culture medium was replaced by 100 μL fresh medium containing 10 μL of 5 mg/mL 3-(4,5- dimethylthiazol-2-yl)-2,5-diphenyltetrazolium bromide (MTT, Sigma–Aldrich, St. Louis, MO, USA) stock solution. After 4 h of labeling the cells with MTT, the medium was replaced with 100 μL dimethyl sulfoxide for 10 min at 37 °C. Samples were mixed and the absorbance was read at 540 nm.

2.2. Co-immunoprecipitation and immunoblotting

Cells were first transfected with pGNMT-FLAG and then treated with DMSO or BaP for 16 h. Cells were rinsed once with cold phosphate buffered saline (PBS) before being lysed in 1 ml of ice-cold buffer (20 mM Tris–Hcl, pH 7.4, 150 mM NaCl, 1% (v/v) Triton X-100, 0.5% (v/v) Nonidet P40, 1 mM EDTA, 1 mM PMSF, 2 μg/ml Antipain C, 50 μg/ml TPCK, 10 μg/ml Leupeptin, 1 mM NaF, 1 mM $NaVO_3$, 5 mM $Na_4P_2O_7$). The 1 mg cell lysates were incubated with the agarose conjugated with an anti-FLAG M2 mAb (anti-FLAG M2 agarose; Sigma) at 4 °C for 4 h. Then the immuoprecipitates were rinsed with TBS buffer (50 mM Tris HCl, 150 mM NaCl, pH 7.4), and analyzed in parallel by 10% SDS–PAGE. An antibody against Flag (1:5000) was used for IP. Western blot procedures were followed as described in a previous report [14]. The following antibodies were used for IB: anti-

FLAG mouse monoclonal antibody (1:5000 dilution; Sigma) and anti-phospho-GNMT serine 9 rabbit polyclonal antibody (1:200 dilution; Yao-Hong Biotechnology). This customized rabbit polyconal pGNMT antibody used a synthetic peptide sequence of "SVYRTRpSLGVAA" and was purchased from Yao-Hong Biotechnology.

2.3. *In-gel digestion*

Each protein sample, obtained from HEK293T cells, was immuoprecipitated with GNMT-flag before applying to the gel, and the locations of proteins were visualized by staining with Coomassie Brilliant Blue G-250 (Bio-Rad, Hercules, CA, USA). After electrophoresis, gel lanes were destained by repeatedly washing in a solution of 25 mM ammonium bicarbonate and 50% (V/V) acetonitrile (1:1) until the protein bands were invisible. After completely being dried with a Speed-Vac (Thermo Electron, Waltham, MA, USA), proteins in the gel fragments were then subjected to the reduction and cysteine alkylation reactions for irreversibly breaking disulfide bridges in the proteins. For the reduction, each gel piece was rehydrated with 2% (V/V) β-mercaptoethanol in 25 mM ammonium bicarbonate and incubated at room temperature for 20 min in the dark. Cysteine alkylation was performed by adding an equal volume of 10% (V/V) 4-vinylpyridine in 25 mM ammonium bicarbonate and 50% (V/V) acetonitrile for 20 min. The samples were than washed by soaking in 1 mL of 25 mM ammonium bicarbonate for 10 min. Following Speed-Vac drying for 20 min, in-gel trypsin digestion was carried out by incubating the samples with 100 ng of modified trypsin (Promega, Mannheim, Germany) in 25 mM ammonium bicarbonate at 37 °C overnight. The supernatant of the tryptic digest was transferred to an Eppendorf tube. Extraction of the remaining peptides from the gel involved adding 25 mM ammonium bicarbonate in 50% (V/V) acetonitrile, then collecting the solution after incubation for 10 min. The resulting digests were dried in a Speed-Vac and stored at −20 °C.

2.4. *Mass spectrometry*

Each tryptic digest sample was re-suspended in 30 μL of 0.1% (V/V) formic acid and analyzed using an online nanoAcquity ultra Performance LC (UPLC) system (Waters, Manchester, UK) coupled to a hybrid linear ion trap Orbitrap (LTQ-Orbitrap Discovery) mass spectrometer with a nanoelectrospray ionization source (Thermo Scientific, San Jose, CA, USA). For reverse phase nano-UPLC-ESI-MS/MS analyses, a sample (2 μL) of the desired peptide digest was loaded into the trapping column (Symmetry C18, 5 μm, 180 μm × 20 mm, Waters) by an autosampler. The reverse phase separation was performed using a linear acetonitrile gradient from 97% buffer A (100% D.I. water/0.1% formic acid) to 95% buffer B (100% acetonitrile/0.1% formic acid) in 100 min using the micropump at a flow rate of approximately 500 nL/min. The separation was performed on a C18 tip column (C18, 1.7 μm, 75 μm × 100 mm, Poly Micro Technologys) using the nano separation system. As peptides were eluted from the micro-capillary column, they were electrosprayed into the ESI-MS/MS with the application of a distal 2.33 kV spraying voltage with heated capillary temperature of 200 °C. Each scan cycle contained one full-scan mass spectrum (*m*/*z* range: 200–1500) and was followed by three data dependent tandem mass spectra. The collision energy of MS/MS analysis was set at 35%.

LC-MS/MS raw data collected by using Xcalibur 2.0.7 SR1 (Thermo Fisher Scientific, San Jose, CA, USA) were converted into peak list files (dta) using the in-house software within a Microsoft VBA environment. The resulting dta files were applied to search against a UniProt protein database with an in-house TurboSequest search server (ver. 27, rev. 11; Thermo Electron, Waltham, MA, USA). The following search parameters were applied: peptide mass tolerance, 0.5 Da; fragment ion tolerance, 1 Da; enzyme set as trypsin; one missed cleavage allowed; peptide charge, 2^+ and 3^+; and oxidation on methionine (+16 Da), vinylpyridine alkylation on cysteine (+105.06 Da) allowed as variable modifications. A protein was identified when at least two unique peptides were matched with the Xcorr score for each peptide >2.5. False-discovery rate (FDR, ≤1%) obtained from the search against the decoy database was used to estimate the protein identifications.

2.5. *Indirect-immunofluorescence antibody assay*

Cultured HEK 293T cells, transfected with plasmids encoding wild type [WT]-GNMT, GNMT serine 9 mutant ($GNMT^{S9A}$) or GNMT threonine 7 mutant ($GNMT^{T7A}$), were placed on cover slides, treated with 10 μM BaP or 0.1%DMSO, fixed with solution I (4% paraformaldehyde and 400 mM sucrose in PBS) at 37 °C for 30 min, fixed with solution II (fixing solution I plus 0.5% Triton X-100) at room temperature for 15 min, and fixed with blocking buffer (0.5% BSA in PBS) at room temperature for 1 h. After washing with PBS, the slides were allowed to react with various primary antibodies at 4 °C overnight. Rabbit anti-GNMT antiserum-R54 (1:200 dilution), FITC-conjugated and Rhodamine-conjugated anti-rabbit IgG were used as secondary antibodies. After four rinses with PBS, slides were mounted and observed using a confocal fluorescence microscope (TCS-NT, Hilden, Germany). DNA was stained with Hoechst H33258 (Sigma–Aldrich) to localize cell nuclei.

2.6. *Quantitative real-time PCR (qRT-PCR)*

RNA was prepared by using Tri Reagent (Sigma–Aldrich, St Louis, MO, USA) and was reverse transcribed into cDNA using a Super Script II Reverse Transcriptase Kit (Invitrogen Inc., Carlsbad, CA, USA). PCR was performed on an ABI StepOne Plus System (Applied Biosystems, Foster City, CA, USA) using the LightCycler® First Start DNA Master SYBR Green I reagent (Roche Diagnostics, Basel, Switzerland). The mRNA level was normalized using the GAPD mRNA level as the standard. The expression profiles of Cyp1a1 and Cyp1a2 mRNA in BaP treated GFP, GNMT or $GNMT^{S9A}$ stable cells were normalized to their DMSO control. The following primers were used: CYP1A1-F (5′-GCTGCAACGGGTGGAATT) and CYP1A1-R (5′-CAGGCATGCTTCATGGTTAGC-3′) for CYP1A1; CYP1A2-F (5′-GGAGCAGGATTTGACACAGTCA-3′) and CYP1A2-R (5′-TTCCTCTGTATCTCAGGCTTGGT-3′) for CYP1A2; GAPD-F (5′-TGGTATCGTGGAAGGACTCA-3′) and GAPD-R (5′-AGTGGGTGTCGCTGTTGAAG-3′) for GAPD.

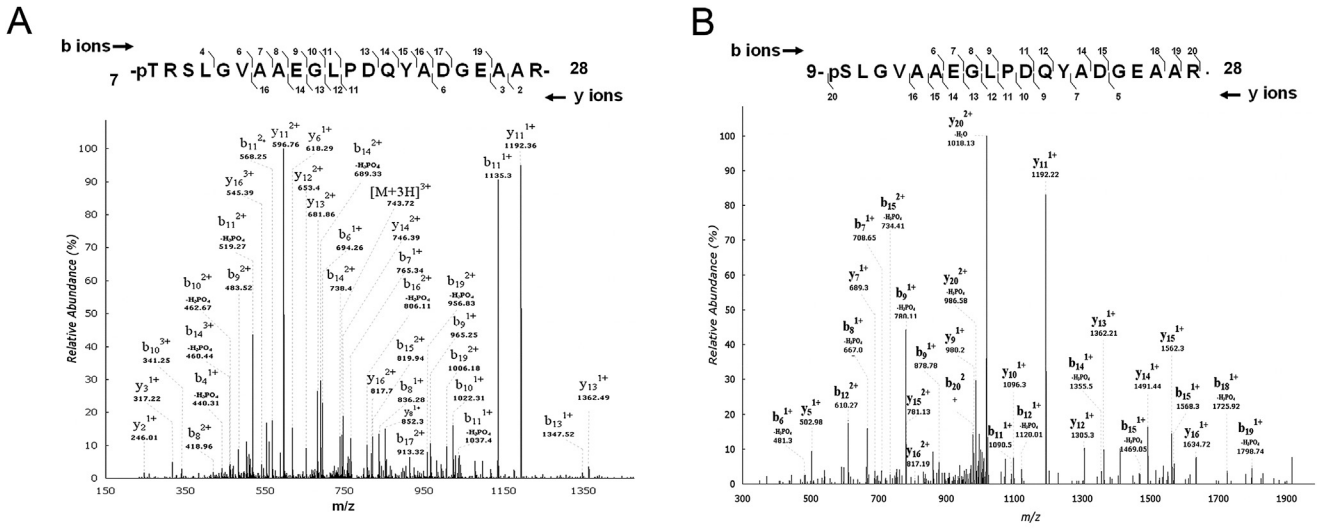

Fig. 1 – MS/MS spectra of identified P-Thr and P-Ser peptides: (A) pTRSLGVAAEGLPDQYADGEAAR from cells treated with DMSO and (B) pSLGVAAEGLPDQYADGEAAR from cells treated with BaP. The experiments were repeated once and similar results were obtained. Representative data are shown.

2.7. *Statistical analysis*

Statistical analyses were performed using MS excel and GraphPad Prism 5.0 software (La Jolla, CA, USA). Cumulative tumor incidence curves were analyzed using the Kaplan–Meier method. p-values were calculated using the unpaired two-sided Student's t-test to compare groups, and $p < 0.05$ was considered statistically significant.

3. Results

3.1. *GNMT nuclear translocation induced by BaP is accompanied with S9 phosphorylation*

It has been reported that benzo(a)pyrene can induce GNMT nuclear translocation [14]. Using mass spectrometric

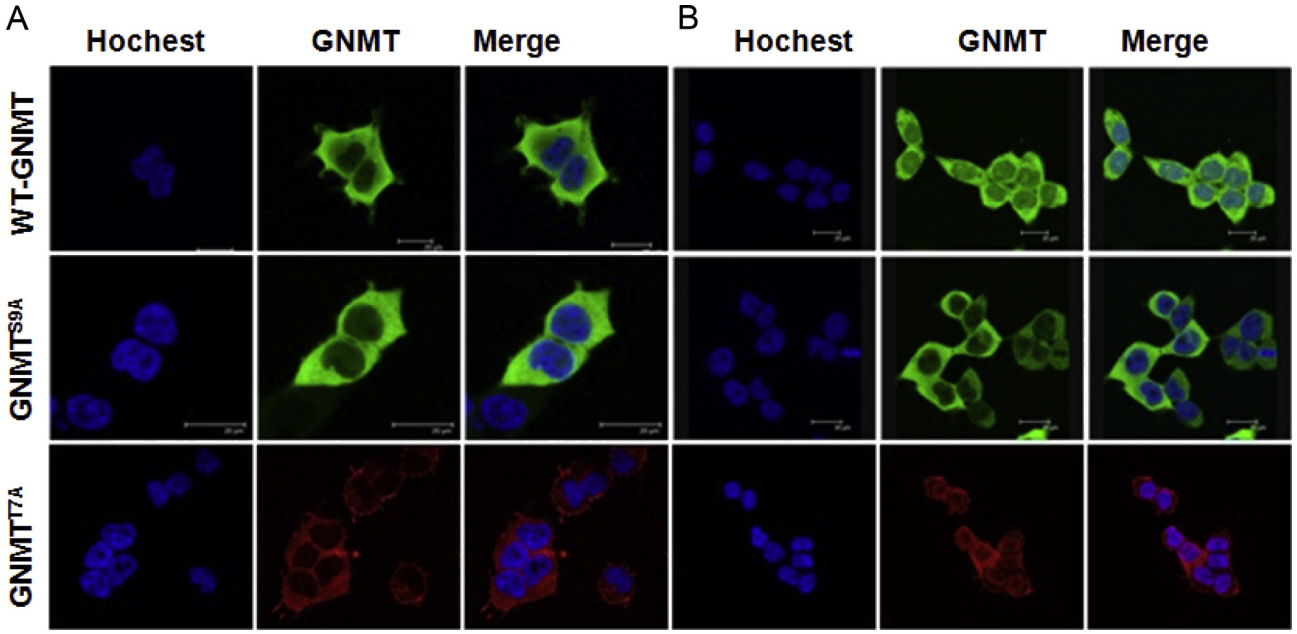

Fig. 2 – Serine 9 mutation abrogates BaP-induced GNMT nuclear translocation. Transfected cells were treated with DMSO (A) or BaP (B) and fixed for Immunofluoresence analysis. GNMT^{S9A} expressing cells were weakly stained in the nucleus after BaP treatment. The experiments were repeated once and similar results were obtained. Representative data are shown.

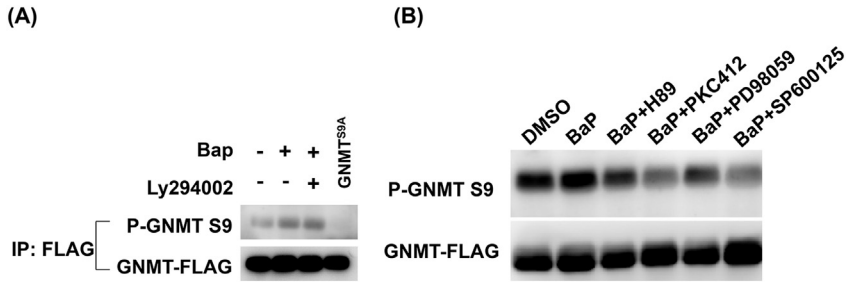

Fig. 3 – PKC and JNK, but not Akt, may be required for GNMT S9 phosphorylation upon BaP treatment. Transfected cells expressing GNMT or S9A mutant were treated with DMSO or BaP with or without the presence of (A) Ly29402 (PI3K inhibitor) or (B) H89 (PKA inhibitor), PKC412 (PKC inhibitor), PD98059 (MEK inhibitor), SP600125 (JNK inhibitor). The experiments were repeated twice and similar results were obtained. Representative data are shown.

techniques we identified phosphorylation sites of GNMT. Fig. 1A presents the P-Thr peptide, pTRSLGVAAEGLPD-QYADGEAAR, obtained from DMSO-treated group. The fragment ion $[b4\text{-}H_3PO_4]^+$ suggested a phosphorylation site on T7. Another phosphopeptide identified as pSLGVAAEGLPD-QYADGEAAR was obtained from BaP-treated group (Fig. 1B). The fragment ions $[b6\text{-}H_3PO_4]^+$ and $[y20\text{-}H_3PO_4]^{2+}$ suggested a phosphorylation site on S9. Our data showed that different amino acid was phosphorylated upon DMSO or BaP treatment.

3.2. *S9 phosphorylation plays a role in GNMT nuclear translocation induced by BaP*

To investigate roles of S9 phosphorylation of GNMT, mutant forms of GNMT were utilized. GNMT serine 9 mutant (GNMT^{S9A}) and GNMT threonine 7 mutant (GNMT^{T7A}) were transiently over-expressed to demonstrate whether S9 phosphorylation is important to BaP-induced nuclear translocation. As shown in Fig. 2, 82% of WT-GNMT expressing cells had nuclear staining pattern upon BaP treatment while only 6% of GNMT^{S9A} expressing cells had weak nuclear staining. The threonine 7 mutation did not show effects on GNMT nuclear translocation after BaP treatment.

In order to have a better recognition of phosphorylated GNMT, a customized rabbit polyclonal P-GNMT S9 antibody was generated. As shown in Figs. S1a and S1b, pS9 GNMT recognized peptides being phosphorylated at S9 and T7-S9. This antibody was applied on samples after immunoprecipitation of GNMT (WT or GNMT^{S9A}) resulting no reactive for GNMT^{S9A}. In addition, a number of inhibitors including Ly29402 (PI3K inhibitor), H89 (PKA inhibitor), PKC412 (PKC inhibitor), PD98059 (MEK inhibitor) and SP600125 (JNK inhibitor) were used to examine the BaP-induced S9 GNMT phosphorylation pathways. Fig. 3B shows that such phosphorylation may be affected by PKC (protein kinase C) and JNK (c-Jun NH2-terminal kinase) inhibitors.

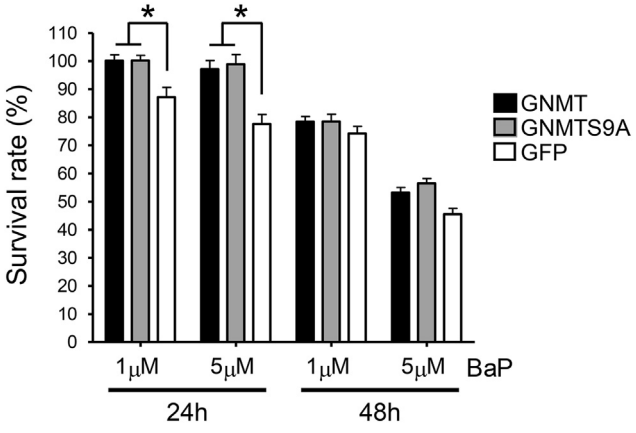

Fig. 4 – S9A mutant of GNMT can antagonize the acute cytotoxic effects of BaP. Transfected cells stably expressing GFP, GNMT or GNMT^{S9A} were treated DMSO or BaP for indicated time period. Data are presented as percentage of viable cells compared with solvent control (DMSO). Each experiment was performed in triplicate. The result showed that S9A mutant of GNMT significantly attenuates BaP-induced acute cytotoxicity as well as wild type GNMT. Results are the means ± SD (n > 3). $^*p < 0.05$.

3.3. *The effects of changing the amino acid of phosphorylation site of GNMT*

Fig. 4 shows that WT GNMT overexpression cells and S9A mutant cells, not GFP overexpression cells, can antagonize the acute cytotoxic effects of BaP for the treatment of 24 h of both 1 and 5 μM of BaP. This effect was not profound when the treatment time was extended to 48 h. This indicates that one amino acid modification may not change the whole protein structure. As a result, the survival rates were unchanged. Interestingly, such mutation enhanced BaP induced Cyp1a expression while WT-GNMT reduced that expression (Fig. 5). There may be a dominant negative phenotype where mutated GNMT binds with endogenous GNMT causing the GNMT homodimeric form unable to function properly.

4. Discussion

Protein post-translational modification (PTM) adds varieties to the proteome through addition, cleavage or degradation of functional groups or subunits. Hundreds of PTMs have been found; phosphorylation, glycosylation, and acetylation are highly experimentally detected PTMs. Among them, phosphoserine and phosphothreonine are the most common ones. Indeed, reversible modifications, such as phosphorylations, have better information processing capabilities [15].

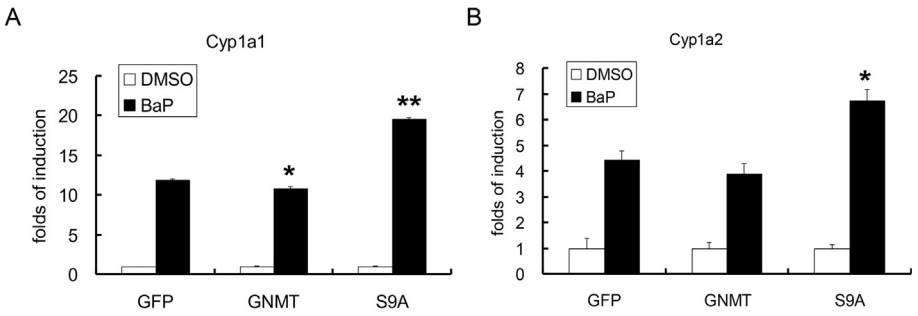

Fig. 5 – S9A mutant of GNMT enhances BaP induced Cyp1a expression. Transfected cells stably expressing GFP, GNMT or GNMT^{S9A} were treated with DMSO or BaP. Compare to GFP-expressing cells, the induction folds of Cyp1a1 and Cyp1a2 by BaP decreased in GNMT -expressing cells, while are significantly enhanced in GNMT^{S9A} stable cells. Results are the means ± SD (n > 3).$^{*}p < 0.05$. $^{**}p < 0.01$.

Phosphorylation is often accompanied by changes in protein function, such as changing the enzyme activity of proteins, the protein distribution within cells or the interactions with other proteins. Besides, it has been demonstrated that phosphorylation plays a role in GNMT translocation from the cytosol to the nucleus [16]. In recent years, the technique of mass spectrometry has been widely used to study protein post-translational modification. Luka and coworkers identified the phosphorylation sites of rat GNMT at serine 9, 71, 182, and 241 [17]. Previously, we reported that GNMT is involved in benzo(*a*)pyrene (BaP) detoxification pathway and being translocated from cell cytoplasm to cell nucleus after BaP treatment [14]. We now identified serine 9 as the BaP-induced phosphorylation site of GNMT. Serine 9, near the N-terminus of GNMT, is likely to affect its enzyme activity and its ability to bind to folic acid since the folate binding site requires 1–7 N-terminal regions from one pair of subunits and 205–218 regions from the other pair of subunits [18]. Furthermore, when mutagenesis technique was applied to mutate serine 9 to alanine, most WT-GNMT expressing cells had nuclear staining pattern upon BaP treatment while only 6% of GNMT^{S9A} expressing cells had weak nuclear staining. The observation, GNMT^{S9A} mutant did not undergo nuclear translocation after BaP treatment, indicates that serine 9 of GNMT is important in BaP-GNMT interactions.

BaP can induce protein instability and affect its function by promoting the phosphorylation of p53 and Rb, causing continuous proliferation, non-stop cell cycle and tumorigenesis [19,20]. After BaP enters the cell, it is metabolized to B(a)PDE. B(a)PDE is involved in a number of signal transduction pathways related to tumor promotion and progression by activating the transcription factor AP-1 to regulate downstream gene expression. This end product activates PI3K [21]. Unlike Li's study, our results showed that GNMT interacted with BaP and such BaP-induced GNMT phosphorylation may be a result of PKC and/or JNK. c-Jun N-terminal kinases (JNKs), also known as stress-activated protein kinases (SAPKs), have been reported to be associated with proliferation, apoptosis, motility, metabolism and DNA repair [22]. Protein kinase C (PKC) comprises a family of serine/threonine kinases and regulates various cellular processes including mitogenesis, proliferation, apoptosis, survival and migration as well as tumorigenesis [23]. Since the metabolites of BaP cause damage to DNA and promote cancer, there is no surprise with finding the involvement of JNK. However, because there are many isoforms of PKCs, the function and the role for PKC in BaP-induced GNMT phosphorylation is unclear at this stage.

The alteration of cell viability was not obvious. Cells expressing GNMT^{WT} and GNMT^{S9A} can resist BaP comparing with those expressing GFP. Since there was only one amino acid change (a hydroxy group removed), the whole protein structure was nearly intact. Nevertheless, cells expressing GNMT^{S9A} showed higher Cyp1a1 and Cyp1a2 mRNA expression upon BaP treatment. This may be due to the dominant negative phenotype of GNMT where the endogenous GNMT^{WT} formed a dimer with GNMT^{S9A}, losing the ability to be phosphorylated and nuclear translocation. As a result, the S9A mutant of GNMT enhanced BaP induced Cyp1a expression.

5. Conclusion

In summary, we identified serine 9 as the required phosphorylation site for GNMT translocation upon BaP treatment. Our results, using molecular biology techniques, demonstrate that this phosphorylation site is associated with nuclear translocation of GNMT. A mutant from of GNMT (S9A mutation) lost the ability of phosphorylation and increased Cyp1a expression upon BaP treatment. In addition, PKC and JNK may be required for such phosphorylation. Further characterization of phosphorylated GNMT for its link to BaP may provide new insights into detoxification mechanism of environmental carcinogens. This may be applied to the development of novel biomarkers for clinical diagnosis as well as for the development of therapeutic or even chemopreventive drugs.

Conflicts of interest

The authors report no conflicts of interest.

Acknowledgments

This work was supported in part by the following grants: Program to Upgrade the R&D Capabilities of Private Universities grant (No. MOST105-2632-B-037-001), Ministry of

Science and Technology of Taiwan (No. MOST104-2320-B-037-031-MY3 and MOST107-2320-B-037-003), Aim for the Top Universities Grant from Kaohsiung Medical University (No. KMU-TP104E11, KMU-TP104E14, KMU-TP104E37 and KMU-TP105E08), Aim for the Top 500 Universities grant from Kaohsiung Medical University (No. KMU-DT105004, KMU-DT106002), KMU Global Networking Talent Plan (No. 105KMUOR02 and 105KMUOR05) and Taiwan Protein Project (No. AS-KPQ-105-TPP). This work was also financially supported by the Research Center for Environmental Medicine, Kaohsiung Medical University, Kaohsiung, Taiwan from The Featured Areas Research Center Program within the framework of the Higher Education Sprout Project by the Ministry of Education (MOE) in Taiwan.

Appendix A. Supplementary data

Supplementary data to this article can be found online at https://doi.org/10.1016/j.jfda.2018.12.007.

REFERENCES

[1] Boström CE, Gerde P, Hanberg A, Jernström B, Johansson C, Kyrklund T, et al. Cancer risk assessment, indicators, and guidelines for polycyclic aromatic hydrocarbons in the ambient air. Environ Health Perspect 2002;110:451–88.
[2] Bull S, Collins C. Promoting the use of BaP as a marker for PAH exposure in UK soils. Environ Geochem Health 2013;35:101–9.
[3] Chen L, Devanesan PD, Higginbotham S, Ariese F, Jankowiak R, Small GJ, et al. Expanded analysis of benzo [a] pyrene-DNA adducts formed in vitro and in mouse skin: their significance in tumor initiation. Chem Res Toxicol 1996;9:897–903.
[4] Miller EC. Some current perspectives on chemical carcinogenesis in humans and experimental animals: presidential address. Cancer Res 1978;38:1479–96.
[5] Xue W, Warshawsky D. Metabolic activation of polycyclic and heterocyclic aromatic hydrocarbons and DNA damage: a review. Toxicol Appl Pharmacol 2005;206:73–93.
[6] Einaudi L, Courbiere B, Tassistro V, Prevot C, Sari-Minodier I, Orsiere T, et al. In vivo exposure to benzo (a) pyrene induces significant DNA damage in mouse oocytes and cumulus cells. Hum Reprod 2013;29:548–54.
[7] Kerr SJ. Competing methyltransferase systems. J Biol Chem 1972;247:4248–52.
[8] Wagner C, Briggs WT, Cook RJ. Inhibition of glycine N-methyltransferase activity by folate derivatives: implications for regulation of methyl group metabolism. Biochem Biophys Res Commun 1985;127:746–52.
[9] Liao YJ, Liu SP, Lee CM, Yen CH, Chuang PC, Chen CY, et al. Characterization of a glycine N-methyltransferase gene knockout mouse model for hepatocellular carcinoma: implications of the gender disparity in liver cancer susceptibility. Int J Cancer 2009;124:816–26.
[10] Yang MH, Chen WJ, Fu YS, Huang B, Tsai WC, Chen YM, et al. Utilizing glycine N-methyltransferasegene knockout mice as a model for identification of missing proteins in hepatocellular carcinoma. Oncotarget 2018;9:442–52.
[11] Chen M, Ho CW, Huang YC, Wu KY, Wu MT, Jeng HA, et al. Glycine N-methyltransferase affects urinary 1-hydroxypyrene and 8-hydroxy-2′-deoxyguanosine levels after PAH exposure. J Occup Environ Med 2011;53:812–9.
[12] Chang MM, Lin CN, Fang CC, Chen M, Liang PI, Li WM, et al. Glycine N-methyltransferase inhibits aristolochic acid nephropathy by increasing CYP3A44 and decreasing NQO1 expression in female mouse hepatocytes. Sci Rep 2018;8:6960.
[13] Yen CH, Hung JH, Ueng YF, Liu SP, Chen SY, Liu HH, et al. Glycine N-methyltransferase affects the metabolism of aflatoxin B1 and blocks its carcinogenic effect. Toxicol Appl Pharmacol 2009;235:296–304.
[14] Chen SY, Lin JR, Darbha R, Lin P, Liu TY, Chen YM. Glycine N-methyltransferase tumor susceptibility gene in the benzo (a) pyrene-detoxification pathway. Cancer Res 2004;64:3617–23.
[15] Prabakaran S, Lippens G, Steen H, Gunawardena J. Post-translational modification: nature's escape from genetic imprisonment and the basis for dynamic information encoding. Wiley Interdiscip Rev Syst Biol Med 2012;4:565–83.
[16] Bhat R, Weaver JA, Wagner C, Bodwell JE, Bresnick E. ATP depletion affects the phosphorylation state, ligand binding, and nuclear transport of the 4 S polycyclic aromatic hydrocarbon-binding protein in rat hepatoma cells. J Biol Chem 1996;271:32551–6.
[17] Luka Z, Ham AJL, Norris JL, Yeo EJ, Yermalitsky V, Glenn B, et al. Identification of phosphorylation sites in glycine N-methyltransferase from rat liver. Protein Sci 2006;15:785–94.
[18] Luka Z, Pakhomova S, Loukachevitch LV, Egli M, Newcomer ME, Wagner C. 5-methyltetrahydrofolate is bound in intersubunit areas of rat liver folate-binding protein glycine N-methyltransferase. J Biol Chem 2007;282:4069–75.
[19] Gao A, Liu B, Shi X, Jia X, Ye M, Jiao S, et al. Phosphatidylinositol-3 kinase/Akt/p70S6K/AP-1 signaling pathway mediated benzo (a) pyrene-induced cell cycle alternation via cell cycle regulatory proteins in human embryo lung fibroblasts. Toxicol Lett 2007;170:30–41.
[20] Tampio M, Loikkanen J, Myllynen P, Mertanen A, Vähäkangas K. Benzo (a) pyrene increases phosphorylation of p53 at serine 392 in relation to p53 induction and cell death in MCF-7 cells. Toxicol Lett 2008;178:152–9.
[21] Li J, Tang MS, Liu B, Shi X, Huang C. A critical role of PI-3K/Akt/JNKs pathway in benzo [a] pyrene diol-epoxide (B [a] PDE)-induced AP-1 transactivation in mouse epidermal Cl41 cells. Oncogene 2004;23:3932–44.
[22] Johnson GL, Nakamura K. The c-jun kinase/stress-activated pathway: regulation, function and role in human disease. Biochim Biophys Acta 2007;1773:1341–8.
[23] Griner EM, Kazanietz MG. Protein kinase C and other diacylglycerol effectors in cancer. Nat Rev Cancer 2007;7:281–94.